Slit between Micro Machined Plates for Observation of Passing Cell: Deformation and Velocity

Shigehiro HASHIMOTO, Yusuke TAKAHASHI, Keisuke KAKISHIMA, Yuki TAKIGUCHI

Biomedical Engineering, Department of Mechanical Engineering,
Kogakuin University, Tokyo, 163-8677, Japan
shashimoto@cc.kogakuin.ac.jp http://www.mech.kogakuin.ac.jp/labs/bio/

ABSTRACT

A micro slit between micro ridges has been used for observation of a biological cell passing through the micro slit *in vitro*. At the middle part of the flow channel, the slit (0.8 mm < width < 2 mm, 0.01 mm height) has been made between the micro ridges on the transparent polydimethylsiloxane plate and the glass plate by photolithography technique. Four kinds of cells were used in the test: C2C12 (mouse myoblast cells), Hepa1-6 (mouse hepatoma cells), MC3T3-E1 (mouse osteoblast precursor cell line), and Neuro-2a (mouse neural crest-derived cell line). The suspension of each kind of cells was injected to the slits. The deformation of cells passing through the micro slit was observed with an inverted phase-contrast microscope. For the reference, the passing speed of the porcine red blood cells through the slit was observed. The experimental results show that cells deform to the flat circular disk and pass through the micro slit. The passing velocity through the slit depends on the deformation ratio of the cell. The designed slit between micro ridges has capability for observation of the deformation and the passing velocity of the single cell.

Keywords: Biomedical Engineering, C2C12, Hepa1-6, Neuro-2a, MC3T3-E1, Photolithography and Micro-slit.

1. INTRODUCTION

The deformability of the biological cell plays an important role *in vivo*. An erythrocyte, for example, has high flexibility, and deforms in the shear flow [1-3]. It also passes through micro-circulation, of which the dimension is smaller than the diameter of the red blood cell. After circulation through the blood vessels for days, the red blood cell is trapped in the micro-circulation systems. A slit is one of the systems, which sorts biological cells *in vivo* [4]. The sorting at the slit depends on the deformability of the cell. Several cells are able to pass very narrow slits.

The photolithography technique enables manufacturing the micro-morphology in the flow channel [5-14]. The behavior of cells in the flow channel will be applied to the cell sorting [9-16]. The photolithography technique can be applied to make a micro slit [5-10]. The slit between micro cylinders was made to sort cells in the previous study [9, 10]. The deformation of the depth direction between cylinders, however, cannot be observed by the conventional optical microscope. To observe the deformed cell at the direction perpendicular to the walls of the slit, the slit is designed with the combination of micro ridges in the present study.

In the present study, a micro slits have been fabricated between micro ridges by the photolithography technique, and deformation of a biological cell passing through the micro slit has been observed *in vitro*.

2. METHODS

Micro Slit

The slit, of which width (w) is 0.8 mm, length (l) is 0.1 mm and height (h) is 0.010 mm, has been designed between a transparent polydimethylsiloxane (PDMS) plate and a borosilicate glass (Tempax) plate [5] (Fig. 1). The upper plate of PDMS has a rectangular ridge of 0.05 mm height, 0.10 mm width, and 2 mm length. The lower plate of glass has a rectangular groove of 0.010 mm depth (h), 2 mm width, and 20 mm length, which has a narrow width (W) part (0.8 mm < W < 2 mm). These plates keep contact to make slits between them. The slit is located at the middle part of the flow channel, which has the following dimension: height of 0.064 mm, width of 2 mm, and length of 30 mm.

Photomask for Upper Plate

The glass plate of 0.2 mm thick was used for the base of the mask. Before the vapor deposition of titanium, the surface of the glass plate was hydrophilized by the oxygen (30 cm^3/min, 0.1 Pa) plasma ashing for five minutes at 100 W by the reactive ion etching system (FA-1, Samco Inc., Kyoto). Titanium was coated on the surface with 150 nm thick in the electron beam vapor deposition apparatus (JBS-Z0501EVC, JEOL Ltd., Japan) at the deposition rate of 0.1 nm/s. The positive photoresist material of OFPR-800LB was coated on the titanium at the disk at 7000 rpm for 60 s with the spin coater (1H-DX2, Mikasa Co. Ltd., Tokyo, Japan). The photoresist was baked on the heated plate at 368 K for five minutes.

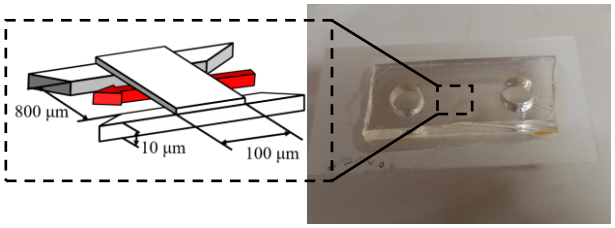

Fig. 1: Microslit in flow channel.

The pattern was drawn on the mask with a laser drawing system (DDB-201K-KH, Neoark Corporation, Hachioji, Japan). To control the dimension of the pattern on the mask with the laser drawing system, the parameters were selected as follows: the voltage of 3.3 V, the velocity of 0.1 mm/s, the acceleration of 0.5 mm/s^2, and the focus offset at +0.1. The pattern was baked on the heated plate at 368 K for five minutes. The photoresist was developed with NMD-3 for 5 minutes. The disk was rinsed by the ultrapure water, and dried by the spin-dryer. The titanium coating disk was etched with the plasma gas (SF_6, Ar) using RIE-10NR (Samco International, Kyoto, Japan). For etching, the gas of SF_6 (50 cm^3/min at 1013 hPa) with Ar (50 cm^3/min at 1013 hPa) was applied at 100 W at 4 Pa for ten minutes. The residual OFPR-800LB was exfoliated by acetone,

Mold for Upper Plate

A glass plate (38 mm × 26 mm × 1 mm: Matsunami Glass Ind., Ltd., Osaka, Japan) is used for a surface mold for the upper disk. The plate was cleaned by an ultrasonic cleaner with alkaline solution, and rinsed by the ultrapure water. The surface of the glass plate was hydrophilized by the oxygen (30 cm^3/min, 0.1 Pa) plasma ashing for five minutes at 100 W by the reactive ion etching system (FA-1). The negative photoresist material of high viscosity (SU8-10: Micro Chem Corp., MA, USA) was coated on the glass plate at 1000 rpm for 30 s with a spin coater. After the photoresist was baked on the heated plate at 338 K for two minutes, the plate was baked on the heated plate at 368 K for seven minutes. SU8-10 was coated on the plate at 1000 rpm for 30 s with a spin coater again. After the photoresist was baked on the heated plate at 338 K for one minutes, the plate was baked on the heated plate at 368 K for five minutes. The photomask was mounted on the surface of SU8-10, and the photoresist was exposed to the UV light through the mask in the mask aligner (M-1S, Mikasa Co. Ltd., Japan) at 15 mW/cm^2 for 20 s. After the photoresist was baked on the heated plate at 338 K for one minute, the plate was baked on the heated plate at 368 K for five minutes. The photoresist was developed with SU-8 developer (Nippon Kayaku Co., Ltd, Tokyo, Japan) for ten minutes. The glass surface with the micro pattern was rinsed with IPA (2-propanol, Wako Pure Chemical Industries, Ltd.) for five minutes, and with the ultrapure water. The plate was dried by the spin-dryer.

Upper Plate

After the mold of the glass plate was enclosed with a peripheral wall of polyimide, PDMS (Sylgard 184 Silicone Elastomer Base, Dow Corning Corporation) was poured together with the curing agent (Dow Corning Corporation) on the mold. The volume ratio of curing agent is ten percent of PDMS. After degassing, PDMS was baked at 373 K for one hour in an oven (DX401, Yamato Scientific Co., Ltd, Tokyo, Japan). The baked plate of PDMS is exfoliated from the mold. The dimension of the ridges on manufactured PDMS was measured with the laser microscope (VK-X200, Keyence Corporation, Osaka, Japan). Two holes of 8 mm diameter were machined with a punching tool at the upper disk to make the inlet and the outlet for the flow channel.

Photomask for Lower Plate

The glass plate of 0.2 mm thick was used for the base of the mask. Before the vapor deposition of titanium, the surface of the glass plate was hydrophilized by the oxygen (30 cm^3/min, 0.1 Pa) plasma ashing for five minutes at 100 W by the reactive ion etching system (FA-1). Titanium was coated on the surface with 150 nm thick in the electron beam vapor deposition apparatus at the deposition rate of 0.1 nm/s. A part of Titanium coating was covered with the polyimide tape to make the flow channel of 2 mm width (narrow part: 0.8 mm width) × 20 mm length. The titanium coating disk was etched with the plasma gas (SF_6, Ar) using RIE-10NR. For etching, the gas of SF_6 (50 cm^3/min at 1013 hPa) with Ar (50 cm^3/min at 1013 hPa) was applied at 100 W at 4 Pa for ten minutes. Afrter the etching, the polyimide tape was exfoliated.

Lower Plate

A glass plate was cleaned by an ultrasonic cleaner with alkaline solution, and rinsed by the ultrapure water. The surface of the glass plate was hydrophilized by the oxygen (30 cm^3/min, 0.1 Pa) plasma ashing for five minutes at 100 W by the reactive ion etching system (FA-1). The negative photoresist material of high viscosity (SU8-10) was coated on the glass plate at 2000 rpm for 30 s with a spin coater. After the photoresist was baked on the heated plate at 338 K for three minutes, the plate was baked on the heated plate at 368 K for seven minutes. The photomask was mounted on the surface of SU8-10, and the photoresist was exposed to the UV light through the mask in the mask aligner (M-1S) at 15 mW/cm^2 for 20 s. After the photoresist was baked on the heated plate at 338 K for one minute, the plate was baked on the heated plate at 368 K for five minutes. The photoresist was developed with SU-8 developer for three minutes. The glass surface was rinsed with IPA for two minutes, and with the ultrapure water. The plate was dried by the spin-dryer. The height of the lower ridge was measured by the stylus profiler (Dektak XT-E, Bruker Corporation).

Flow Channel

The upper plate of PDMS was rinsed with IPA, and with the ultrapure water. The plate was dried by the spin-dryer. The surface of the PDMS plate was hydrophilized by the oxygen (30 cm^3/min, 0.1 Pa) plasma ashing for thirty seconds at 50 W by the reactive ion etching system (FA-1). The plate was rinsed with APTES (Aminopropyltriethoxysilane) for five minutes, and with the ultrapure water. The plate was dried in the oven at 338 K for three minutes. The upper plate of PDMS was adhered on the lower plate of SU8-10, and was baked on the heated plate at 338 K for five minutes.

Flow Test

Four kinds of cells (passage < 10) were used in the flow test: Hepa1-6 (mouse hepatoma cell line of C57L mouse), C2C12 (mouse myoblast cell line originated with cross-striated muscle of C3H mouse), MC3T3-E1 (an osteoblast precursor cell line derived from Mus musculus (mouse) calvaria), and Neuro-2a (a mouse neural crest-derived cell line). D-MEM (Dulbecco's Modified Eagle Medium) was used for the medium, except αMEM for MC3T3-E1. Each medium contains 10% FBS (decomplemented fetal bovine serum) and 1% penicillin/ streptomycin (GIBCO, Life Technologies Japan Ltd., Tokyo, Japan).

The cells were exfoliated from the bottom of the culture dish with trypsin, and suspended in the culture medium (1000 cells/cm^3). In the case of porcine red blood cells, the blood collected through the carotid artery was diluted by thousand times with the saline solution. The bovine serum albumin solution was prefilled in the flow channel, and incubated for ten minutes at 310 K in the incubator.

The suspension of the cells was poured at the inlet of the flow channel. The suspension flows by the pressure head of 5 mm, which makes the pressure difference of 49 Pa between the inlet and the outlet. The flow rate decreases gradually with the decrease of the pressure head. The behavior of cells near the slit was observed with an inverted phase-contrast microscope (IX71, Olympus Co., Ltd., Tokyo) (Fig. 2).

The microscopic images of thirty frames per second at the shutter speed of 1/2000 s were captured by a camera (DSC-RX100M4, Sony Corporation, Tokyo, Japan). At the images, the outline of each cell was traced with "Image J", and the projected area (A) was calculated. The deformation ratio (Ra) was calculated at each cell by Eq. 1.

$$Ra = A_2 / A_1 \quad (1)$$

In Eq. 1, A_1 is the area before the slit, and A_2 is the area in the slit. Ra is unity, when the area in the slit (A_2) is equal to that before the slit (A_1).

The velocity of the cell passing through the slit (v) was calculated at the movie by "Kinovea". Most of cells pass through the slit in a few seconds, and Data of clogging cell in the slit are not included in the following figures.

The velocity ratio (Rv) was calculated at each cell by Eq. 2.

$$Rv = (v_2 - v_1)/ v_1 \quad (2)$$

In Eq. 2, v_1 is the velocity before the slit, and v_2 is the velocity in the slit. Rv is zero, when the velocity in the slit (v_2) is equal to that before the slit (v_1).

3. RESULTS

The tracing across the ridge on the lower disk measured by the stylus profiler shows that the height of the ridge is 0.010 mm. Fig. 3 exemplifies the tracing across the ridge on the upper disk. The tracing shows that the height of the ridge is 0.06 mm. Fig. 4 exemplifies the microscopic image near the slit. Some cells are stopping at the inlet of the slit. Others are passing through the slit. Fig. 5 exemplifies C2C12 (in red circle) passing through slit. The cell is approaching to the slit (a), enters to the slit (b), is passing through the slit (c), and is leaving from the slit (d).

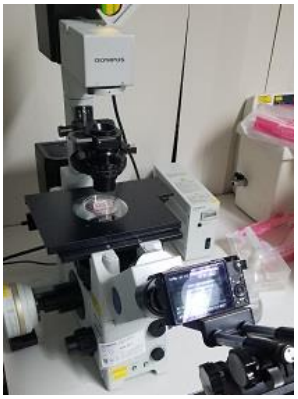

Fig. 2: Experimental system: channel, microscope, camera.

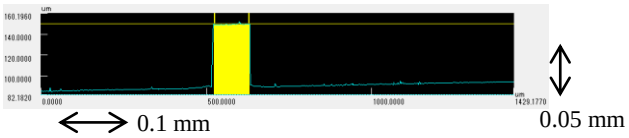

Fig. 3: Tracing across ridge on upper disk: unit, μm.

Fig. 4: Cells passing through slit: dimension from left to right is 0.8 mm; flow direction is from left to right.

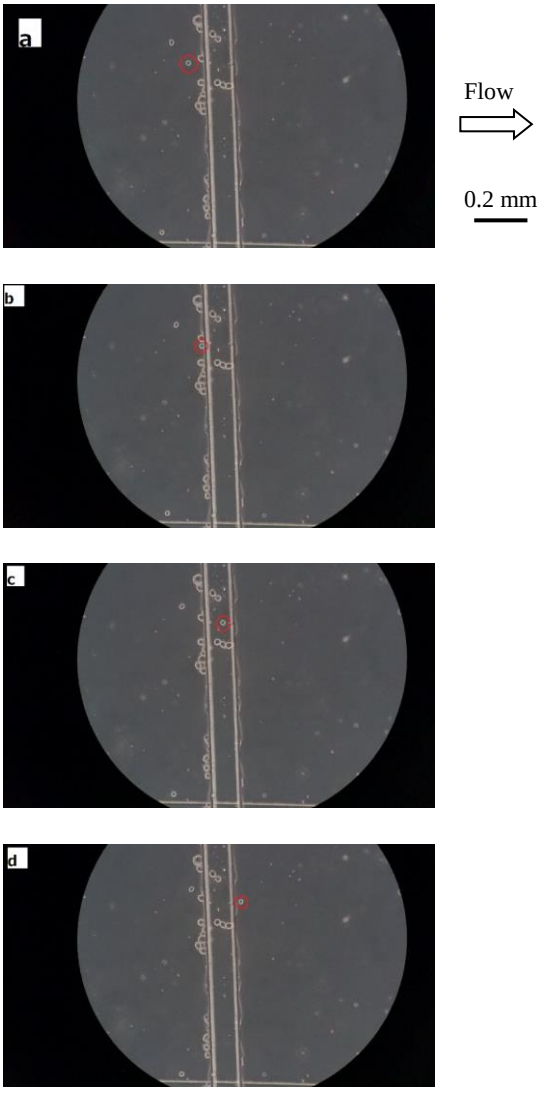

Fig. 5: C2C12 (in red circle) passing through slit: dimension from left to right is 2 mm: approaching to slit (a), passing through slit (c), departing from slit (d).

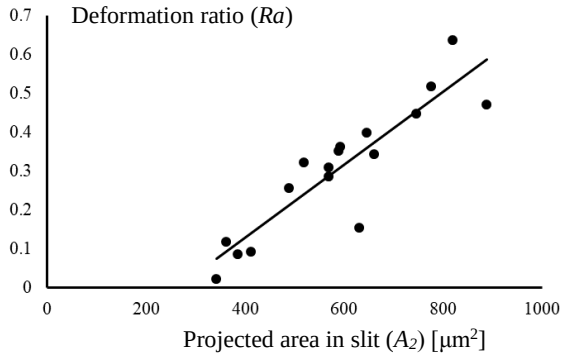

Fig. 6: Relationship between deformation ratio (*Ra*) and area in slit (A_2) of each cell: Neuro-2a.

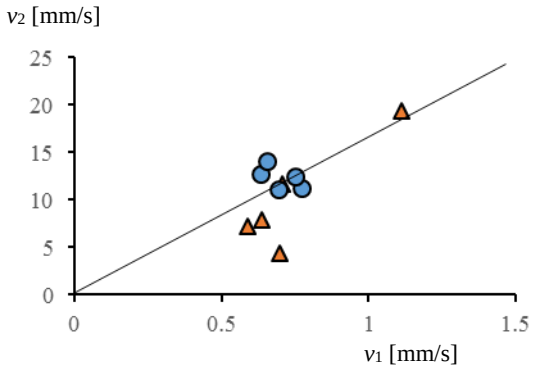

Fig. 7: Velocity of red blood cell before slit (v_1) vs. in slit (v_2): at middle of slit (circle), at fringe of slit (triangle).

Fig. 6 shows the relationship between the deformation ratio (*Ra*) and the projected area in the slit (A_2) of each cell. The line shows the approximate linear relationship by the least squares method. Data scatters, but the bigger cell of the larger area (A_1) makes the larger area in the slit (A_2) with the higher deformation ratio (*Ra*). The approximate line shows that the mean area of the cell before slit (A_1) is 300 μm^2.

Fig. 7 shows the relationship between the velocity of each porcine red blood cell before slit (v_1) and that in slit (v_2). The data of circles show the velocity at middle of slit, and those of triangles show the velocity at fringe of slit. The line shows the linear relationship between v_1 and v_2, which is inversely proportional to the cross sectional area of the flow pass. The ratio of the cross sectional area between the flow channel (0.064 mm height × 2 mm width) and the slit (0.01 mm height × 0.8 mm width) is 16. The velocities of some cells in the fringe area of the slit (v_2) are slightly slower than the linear relationship between v_1 and v_2, which corresponds to the reduced flow velocity in the fringe area in the slit.

Figs. 8-10 show the projected area (Fig. 8a, Fig. 9a, and Fig. 10a) and the velocity (Fig. 8b, Fig. 9b, and Fig. 10b) of each cell: C2C12 (Fig. 8), Hepa1-6 (Fig. 9), and MC3T3-E1 (Fig. 10), respectively. In these figure, each mark of circle and of rhombus shows datum before the slit and in the slit, respectively. Data are arranged in the ascending order of the data before the slit (A_1, v_1). The datum on the each cell is arranged at the corresponding cell number. The projected area (A_2) scatters, but tends to increase with the increase of A_1, which proportionally relates to the size of the cell (Figs. 8a, 9a, and 10a). At the most of cells of Hepa1-6, the velocity of the cell in the slit is much lower than that before the slit (Fig. 9b). At C2C12, the velocity of the cell in the slit is lower than that before the slit especially in the case of the higher velocity before the slit (v_1 > 1 mm/s) (Fig. 8b). At MC3T3-E1, on the other hand, the velocity of the cell in the slit is sometimes higher than that before the slit (Fig. 9b), even at the higher velocity before the slit (v_1 > 0.8 mm/s).

Data of the projected area of each cell are collected in Fig.11 accroding to the kind of cells. The black column shows the mean area before the slit (A_1), and the white column shows the mean area in the slit (A_2). Each bar shows the standard deviation of each mean value. The area is relatively smaller at MC3T3-E1, which corresponds to the smaller size of the cell.

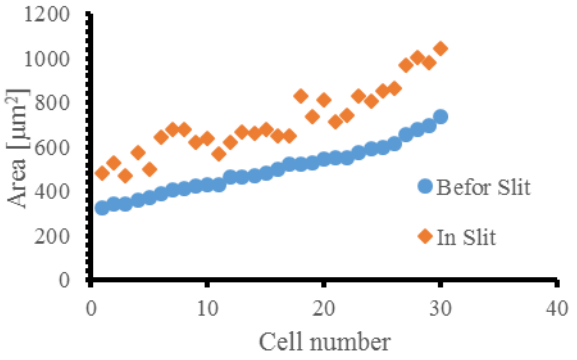

Fig. 8a: Area of C2C12: before slit (circle), in slit (rhombus).

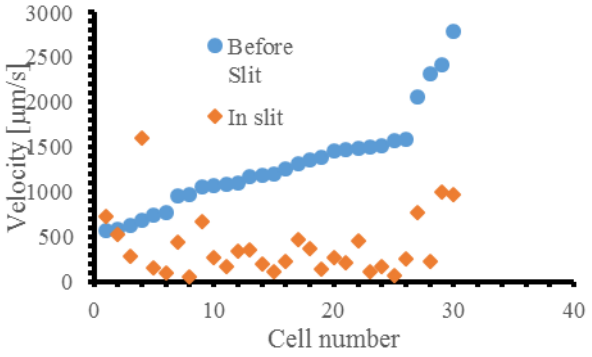

Fig. 8b: Velocity of C2C12: before slit (circle), in slit (rhombus).

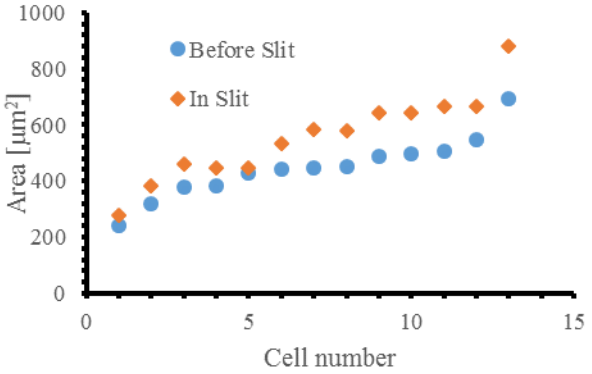

Fig. 9a: Area of Hepa1-6: before slit (circle), in slit (rhombus).

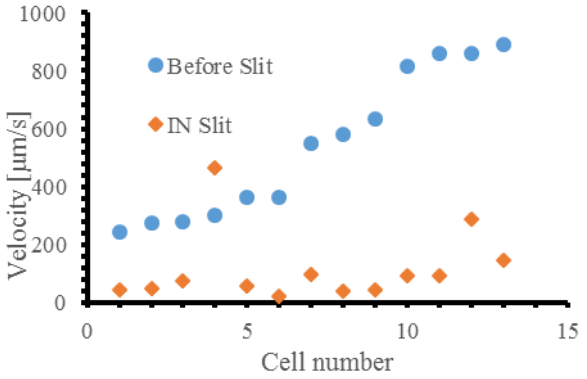

Fig. 9b: Velocity of Hepa1-6: before slit (circle), in slit (rhombus).

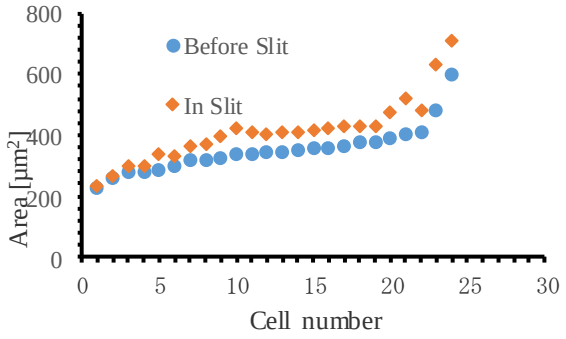

Fig. 10a: Area of MC3T3-E1: before slit (circle), in slit (rhombus).

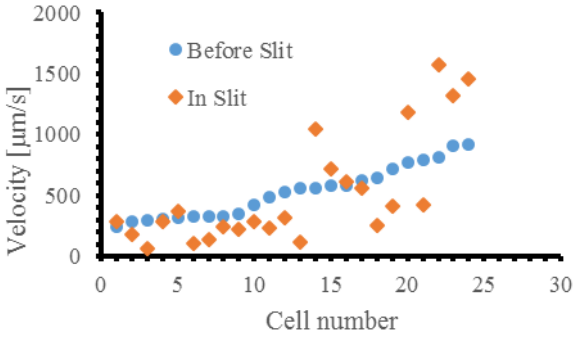

Fig. 10b: Velocity of MC3T3-E1: before slit (circle), in slit (rhombus).

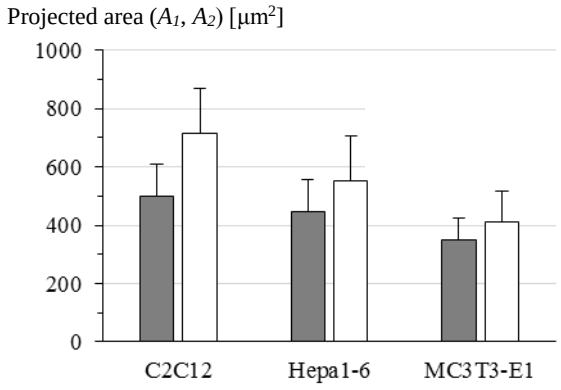

Fig. 11: Projected area of cell: before slit (black), in slit (white): mean (column), standard deviation (bar).

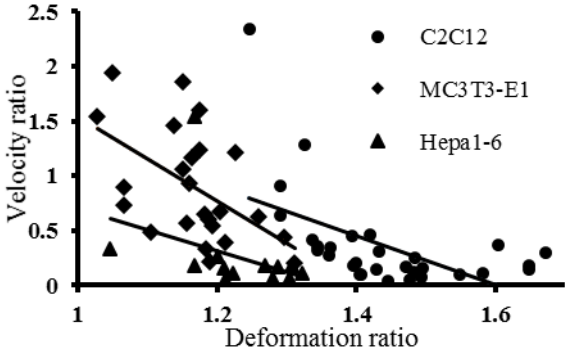

Fig. 12: Relationship between velocity ratio (*Rv*) and deformation ratio (*Ra*): C2C12 (circle), Hepa1-6 (triangle), MC3T3-E1 (rhombus).

Fig. 12 shows the relationship between the velocity ratio (*Rv*) and the deformation ratio (*Ra*). Data are categorized according to the kind of cells: C2C12 (circle), Hepa1-6 (triangle), and MC3T3-E1 (rhombus). The line shows the approximate linear relationship by the least squares method at each kind of cells. As the deformation ratio increases, the velocity ratio decreases. The tendency is remarkable at MC3T3-E1. Every velocity ratio is lower than 3 in Fig. 12. Every velocity ratio of red blood cell on the other hand, is higher than five (Fig. 7).

4. DISCUSSION

When the diameter of the sphere is same as the height of the slit (d = 10 μm), the projected area (A) is 79 μm^2. In Figs. 8-10, the projected area of each cell before the slit (A_1) exceeds 200 μm^2, so that the height of the slit is small enough to make deformation of each cell, which is passing through the slit. The dimension of the width of the slit has been selected wider than 0.8 mm, which is enough wide for a cell to pass through. The wider width of the slit has possibility to make deformation of the wall, which cannot keep precise dimension of the slit [5]. The ridge of the PDMS has elasticity, so that the micro ridge may deform with the small ratio. The reduced velocity of the porcine red blood cell at the fringe area of the slit might correspond to the reduced cross sectional area or the side wall effect (Fig. 7). The velocity ratio in Fig. 12 is smaller than 5, which depends on the friction between the cell and the wall of the slit. The cell of the larger diameter is forced to be deformed at the higher deformation ratio in the slit (Fig. 6). The higher deformation ratio makes the larger projected area in the slit. The higher deformation ratio might increases the frictional resistance at the slit (Fig. 13).

The fine architecture of the red pulp of the spleen has been investigated in the previous study [4]. In the previous studies, the typical micro channel has cylindrical shape with 0.005 mm diameter, which simulates the blood vessel capillary. The red blood cell, on the other hand, passes through micro slit narrower than 0.001 mm in the spleen. The deformability of erythrocyte changes with aging [1]. The deformation is evaluated with the ratio of the projected area of the disk during the passing through the slit in the present study. The deformation in the perpendicular direction can be observed with slit between micro cylindrical pillars [9, 10].

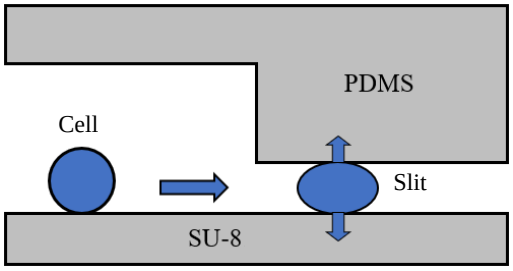

Fig. 13: Cell deformation in slit between plates of PDMS and of SU-8.

Reynolds number (*Re*) is calculated by Eq. 3.

$$Re = \rho\, v\, w/\, \eta \qquad (3)$$

In Eq. 3, ρ is density of the fluid, and q is the flow rate. *Re* is 1, when ρ, v, w, and η are 10^3 kg m^{-3}, 1×10^{-3} m/s, 2×10^{-3} m, and 2×10^{-3} Pa s, respectively. The turbulent flow may not occur in the flow of small value of Reynolds number.

5. CONCLUSION

A micro slit between micro ridges has been used for observation of a biological cell passing through the micro slit *in vitro*. At the middle part of the flow channel, the slit (0.8 mm < width < 2 mm, 0.01 mm height) has been made between the micro ridges on the transparent polydimethylsiloxane plate and the glass plate by photolithography technique. Four kinds of cells were used in the test: C2C12 (mouse myoblast cells), Hepa1-6 (mouse hepatoma cells), MC3T3-E1 (mouse osteoblast precursor cell line), and Neuro-2a (mouse neural crest-derived cell line). For the reference, the passing speed of the porcine red blood cells through the slit was observed. The experimental results show that the passing velocity through the slit depends on the deformation ratio of the cell. The designed slit between micro ridges has capability for observation of the deformation and the passing velocity of the single cell.

6. ACKNOWLEDGMENT

This work was supported by a Grant-in-Aid for Strategic Research Foundation at Private Universities from the Japanese Ministry of Education, Culture, Sports and Technology.

REFERENCES

[1] S. Hashimoto, H. Otani, H. Imamura, et al., "Effect of Aging on Deformability of Erythrocytes in Shear Flow", **Journal of Systemics Cybernetics and Informatics**, Vol. 3, No. 1, 2005, pp. 90-93.

[2] S. Hashimoto, "Detect of Sublethal Damage with Cyclic Deformation of Erythrocyte in Shear Flow", **Journal of Systemics Cybernetics and Informatics**, Vol. 12, No. 3, 2014, pp. 41-46.

[3] A.W.L. Jay, "Viscoelastic Properties of the Human Red Blood Cell Membrane: I. Deformation, Volume Loss, and Rupture of Red Cells in Micropipettes", **Biophysical Journal**, Vol. 13, No. 11, 1973, pp. 1166-1182.

[4] L.T. Chen and L. Weiss, "The Role of the Sinus Wall in the Passage of Erythrocytes through the Spleen", **Blood**, Vol. 41, No. 4, 1973, pp. 529-537.

[5] Y. Takahashi, S. Hashimoto, A. Mizoi and H. Hino, "Deformation of Cell Passing through Micro Slit between Micro Ridges Fabricated by Photolithography Technique", **Proc. 21st World Multi-Conference on Systemics Cybernetics and Informatics**, Vol. 2, 2017, pp. 239-244.

[6] A. Mizoi, Y. Takahashi, H. Hino, S. Hashimoto and T. Yasuda, "Deformation of Cell Passing through Micro Slit between Micro Ridges", **Proc. 20th World Multi-Conference on Systemics Cybernetics and Informatics**, Vol. 2, 2016, pp. 129-134.

[7] A. Mizoi, Y. Takahashi, H. Hino, S. Hashimoto and T. Yasuda, "Deformation of Cell Passing through Micro Slit", **Proc. 19th World Multi-Conference on Systemics Cybernetics and Informatics**, Vol. 2, 2015, pp. 270-275.

[8] S. Hashimoto, A. Mizoi, H. Hino, K. Noda, K. Kitagawa and T. Yasuda, "Behavior of Cell Passing through Micro Slit", **Proc. 18th World Multi-Conference on Systemics Cybernetics and Informatics**, Vol. 2, 2014, pp. 126-131.

[9] Y. Takahashi, S. Hashimoto, H. Hino and T. Azuma, "Design of Slit between Micro Cylindrical Pillars for Cell Sorting", **Journal of Systemics, Cybernetics and Informatics**, Vol. 14, No. 6, 2016, pp. 8-14.

[10] S. Hashimoto, T. Horie, F. Sato, T. Yasuda and H. Fujie, "Behavior of Cells through Micro Slit", **Proc. 17th World Multi-Conference on Systemics Cybernetics and Informatics**, Vol. 1, 2013, pp. 7-12.

[11] Y. Takahashi, S. Hashimoto, H. Hino, A. Mizoi and N. Noguchi, "Micro Groove for Trapping of Flowing Cell", **Journal of Systemics, Cybernetics and Informatics**, Vol. 13, No. 3, 2015, pp. 1-8.

[12] S. Hashimoto, Y. Takahashi, H. Hino, R. Nomoto and T. Yasuda, "Micro Hole for Trapping Flowing Cell", **Proc. 18th World Multi-Conference on Systemics Cybernetics and Informatics**, Vol. 2, 2014, pp. 114-119.

[13] S. Hashimoto, R. Nomoto, S. Shimegi, F. Sato, T. Yasuda and H. Fujie, "Micro Trap for Flowing Cell", **Proc. 17th World Multi-Conference on Systemics Cybernetics and Informatics**, Vol. 1, 2013, pp. 1-6.

[14] S. Hou, H. Zhao, L. Zhao, Q. Shen, K.S. Wei, D.Y. Suh, A. Nakao, M.A. Garcia, M. Song, T. Lee, B. Xiong, S.C. Luo, H.R. Tseng and H.H. Yu, "Capture and Stimulated Release of Circulating Tumor Cells on Polymer-Grafted Silicon Nanostructures", **Advanced Materials**, Vol. 25, No. 11, 2013, pp. 1547-1551.

[15] B. Lincoln, H.M. Erickson, S. Schinkinger, F. Wottawah, D. Mitchell, S. Ulvick, C. Bilby and J. Guck, "Deformability-Based Flow Cytometry", **Cytometry**, Part A: the journal of the International Society for Analytical Cytology, Vol. 59, No.2, 2004, pp. 203-209.

[16] C.L. Chaffer and R.A. Weinberg, "A Perspective on Cancer Cell Metastasis", **Science**, Vol. 331, No. 6024, 2011, pp. 1559-1564.